REPORT DOCUMENTATION PAGE

Form Approved OMB No. 0704-0188

1. REPORT DATE *(DD-MM-YYYY)*	2. REPORT TYPE	3. DATES COVERED *(From – To)*
17-11-2006	Final Report	28 January 2006 - 13-May-10

4. TITLE AND SUBTITLE

-High order numerical schemes for Lattice Boltzmann models: Applications to flows with variable Knudsen

5a. CONTRACT NUMBER
FA8655-05-M-4008

5b. GRANT NUMBER

5c. PROGRAM ELEMENT NUMBER

6. AUTHOR(S)

Dr. Victor Sofonea

5d. PROJECT NUMBER

5d. TASK NUMBER

5e. WORK UNIT NUMBER

7. PERFORMING ORGANIZATION NAME(S) AND ADDRESS(ES)

Romanian Academy of Sciences
Bd. Mihai Viteazul 24
Timisoara 1900
Romania

8. PERFORMING ORGANIZATION REPORT NUMBER

N/A

9. SPONSORING/MONITORING AGENCY NAME(S) AND ADDRESS(ES)

EOARD
Unit 4515 BOX 14
APO AE 09421

10. SPONSOR/MONITOR'S ACRONYM(S)

11. SPONSOR/MONITOR'S REPORT NUMBER(S)
SPC 05-4008

12. DISTRIBUTION/AVAILABILITY STATEMENT

Approved for public release; distribution is unlimited. (approval given by local Public Affairs Office)

13. SUPPLEMENTARY NOTES

14. ABSTRACT

This report results from a contract tasking Romanian Academy of Sciences as follows: The Grantee will inverigate the development of higher order numerical methods to solve Lattice Boltzmann equations, a system of hyperbolic pde's obtained from the Boltzmann Equation by discretizing the collision integrals appearing in the latter system.

15. SUBJECT TERMS
EOARD, Finite Difference Methods, Kinetic Theory, Computational Fluid Dynamics (CFD), CFD

16. SECURITY CLASSIFICATION OF:			17. LIMITATION OF ABSTRACT	18, NUMBER OF PAGES	19a. NAME OF RESPONSIBLE PERSON
a. REPORT	b. ABSTRACT	c. THIS PAGE			SURYA SURAMPUDI
UNCLAS	UNCLAS	UNCLAS	UL	29	19b. TELEPHONE NUMBER *(Include area code)* +44 (0)1895 616021

Center of Fundamental and Advanced Technical Research
Romanian Academy – Timişoara Branch
Bd. Mihai Viteazul 24, RO – 300223 Timişoara, Romania

High order numerical schemes for lattice Boltzmann models: Applications to flow with variable Knudsen number

Contract FA8655–05–M–4008

European Office of Aerospace Research and Development

Item #0003: Final Report

July 10, 2006

Research team:

dr. Victor Sofonea, Principal Investigator

Artur Cristea, PhD student

Contents

1 Pressure - driven microchannel flow

1.1 Introduction

As mentioned in our previous reports [1, 2], Lattice Boltzmann (LB) models [3, 4, 5, 6] are effective for problems where both mesoscopic dynamics and microscopic statistics become important, as in the case of micro - channel flows [7, 8, 9, 10, 11, 12, 13]. In this report, we further investigate the applications of the two-dimensional ($2D$) thermal finite difference Lattice Boltzmann (FDLB) model introduced in [14]. For convenience, a brief description of this model is provided below.

Lattice Boltzmann (LB) models provide an alternative to particle-based models like Molecular Dynamics (MD) or Direct Simulation Monte Carlo (DSMC), as well as to numerical techniques of Computational Fluid Dynamics (CFD) derived from the principles of continuous media mechanics. The development of Lattice Boltzmann models for the investigation of flow phenomena at non-negligible Knudsen numbers [15, 16, 17, 18, 19, 20, 21, 22, 23, 24, 25, 26] has recently received considerable attention due to the increasing interest for mastering gas flow at two extreme scales [7, 8, 9, 10, 11, 12, 13]: high-altitude aerodynamics and micro-electro-mechanical systems (MEMS). Unfortunately, the majority of LB models developed up to date for the investigation of fluid flow at finite Knudsen numbers still refer to the isothermal case.

In the previous reports [1, 2] we approach the non-isothermal gas flow in microchannels using the two-dimensional finite difference LB model with multiple speeds of Watari and Tsutahara [14], which allows the correct recovery of mass, momentum and energy equations of a compressible fluid. The model involves a set of 33 nondimensionalized velocities $\{\mathrm{e}_{00},\, \mathrm{e}_{ki}\}$, $(k = 1, \ldots 4,\ i = 1, \ldots 8)$

$$\mathrm{e}_{00} \;=\; 0 \qquad , \qquad \mathrm{e}_{ki} \;=\; \left[\cos \frac{\pi(i-1)}{4}, \quad \sin \frac{\pi(i-1)}{4} \right] c_k \tag{1}$$

with $c_k \in \{1.0,\, 1.92,\, 2.99,\, 4.49\}$. The corresponding distribution functions $f_{00} = f_{00}(\mathbf{x}, t)$, $f_{ki} = f_{ki}(\mathbf{x}, t)$, evolve according to the non-dimensionalized equations

$$\partial_t f_{ki} + \mathbf{e}_{ki} \cdot \nabla f_{ki} = -\frac{1}{\tau} \left[f_{ki} - f_{ki}^{eq} \right] \tag{2}$$

Here we use the density-dependent relaxation time $\tau = \Lambda / n\bar{c}$, where Λ is a dimensionless constant, $n = n(\mathbf{x}, t)$ is the particle number density and $\bar{c}$ is the local average speed of fluid particles [27]. The equilibrium distribution functions in eqs. (2)

$$f_{ki}^{eq} = f_{ki}^{eq}(\mathbf{x}, t) = n F_k s_{ki} \tag{3}$$

are expressed using the series expansion $s_{ki} = s_{ki}(\theta, \mathbf{u})$ up to fourth order with respect to the Cartesian components u_α ($\alpha = 1,\, 2$) of the fluid velocity (summation over repeated Greek indices is understood):

$$\begin{aligned} s_{ki} \;=\; & \left(1 - \frac{u^2}{2\theta} + \frac{u^4}{8\theta^2} \right) + \frac{1}{\theta} \left(1 - \frac{u^2}{2\theta} \right) e_{ki\xi} u_\xi \;+\; \frac{1}{2\theta^2} \left(1 - \frac{u^2}{2\theta} \right) e_{ki\xi} e_{ki\eta} u_\xi u_\eta \\ + \;& \frac{1}{6\theta^3} e_{ki\xi} e_{ki\eta} e_{ki\zeta} u_\xi u_\eta u_\zeta \;+\; \frac{1}{24\theta^4} e_{ki\xi} e_{ki\eta} e_{ki\zeta} e_{ki\chi} u_\xi u_\eta u_\zeta u_\chi \end{aligned} \tag{4}$$

The weight factors $F_k = F_k(\theta)$ in eq. (3) depend on the local temperature $\theta = \theta(\mathbf{x}, t)$ and the speeds c_k, $k = 1, \ldots 4$. We refer the reader to the literature [1, 2, 14, 27, 28] for further details on the thermal LB model.

1.2 Boundary conditions

1.2.1 Walls

The thermal LB model, as originally developed by its authors [14], uses the second order upwind finite difference scheme to solve the LB evolution equations (2) in the nodes of a two-dimensional square lattice. The boundary nodes were located on the channel walls and an extrapolation method was used to provide the corresponding values of the distribution functions. This procedure forces the fluid's temperature and velocity in the boundary nodes to equal the wall's temperature and velocity. Appropriate boundary conditions [15, 16, 17, 18, 19, 20, 21, 22, 23, 24, 25, 26], many of them based on the concept of diffuse reflection, which dates back to the time of Maxwell and Smoluchowski [29, 30, 31, 32], were already introduced in the isothermal LB models to capture the fluid velocity slip near the walls when the Knudsen number is no longer negligible.

To reduce numerical errors, the MCD flux limiter finite difference scheme [33, 34, 35] is used in our simulations. A first implementation of diffuse reflection boundary conditions in the thermal LB model of Watari and Tsutahara relies on the redistribution (thermalization) of the particle distribution functions in the ghost nodes outside the walls [27]. Although successful in capturing the temperature jump and slip velocity in Couette flow, this implementation of the diffuse reflection boundary conditions does not allow the fluid density to vary along the channel walls, as happens in the case of pressure-driven gas flow. To overcome this drawback, in the previous report [2] we managed the distribution functions to mix (redistribute) themselves in wall nodes instead of ghost nodes. More precisely, the distribution functions whose corresponding velocities point to the wall in the normal direction mix separately from those distribution functions with corresponding velocities orientated along the diagonals of the square lattice. For convenience, we refer to the left wall of the vertical channel in Figure 1, where the black squares $(j = 1/2, l)$ and $(j = 1/2, l + 1/2)$, $l = 0, 1, \ldots$, denote the mixing points on the wall. The corresponding (unknown) values of the particle number density are $n_w^{1/2,l+1/2}$ and $n_w^{1/2,l+1}$, respectively. Although the mixing points may have different temperatures, in this paper we restrict ourselves to the case when the channel wall temperature is constant ($\theta_w^{1/2,l} = \theta_w^{1/2,l+1/2} = \theta_w$, for all l).

In the finite difference LB model we need appropriate procedures to compute the values of the distribution functions $f_{k2}^{0,l}$, $f_{k8}^{0,l+1}$, $f_{k1}^{0,l+1}$ $(l = 0, 1, \ldots)$ defined in the ghost nodes outside the left wall of velocity $\mathbf{u}_w$ [27]. The requirement that the distribution functions follow the Maxwellian distribution law at the mixing points on the left wall

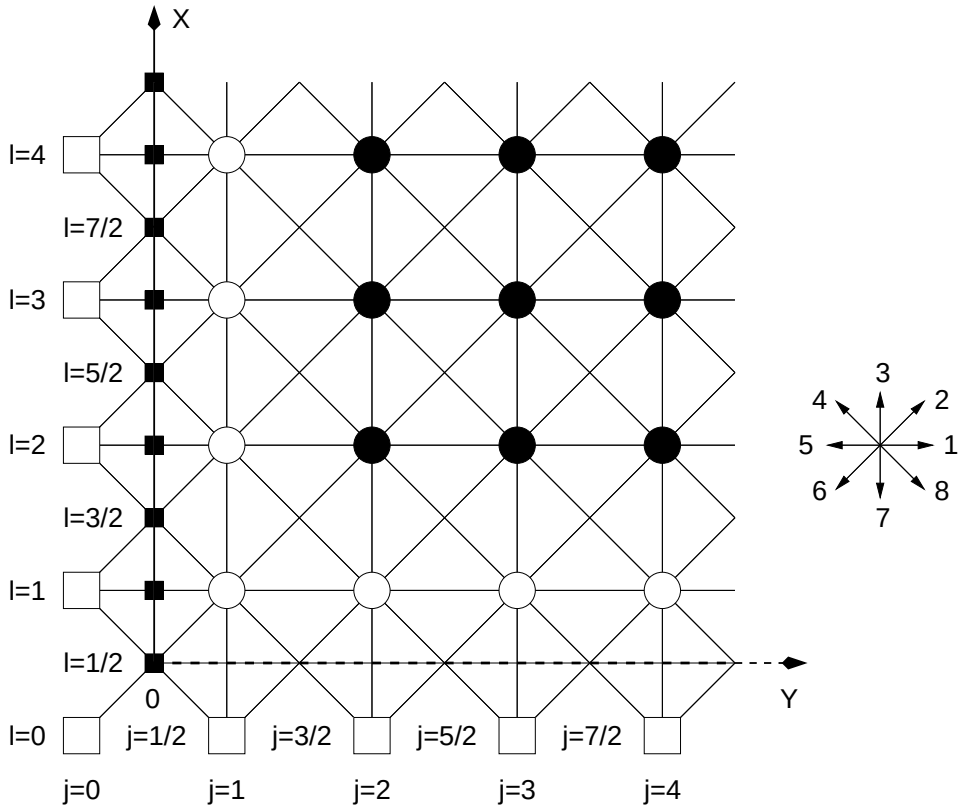

Figure 1: Implementation of diffuse reflection boundary conditions in the lattice nodes near the lower left end of a vertical channel (the dashed line marks the outflow boundary): • - bulk nodes, ∘ - boundary nodes, □ - ghost nodes, ■ - wall nodes where the distribution functions f_{ki}^{jl} follow the Maxwellian distribution.

reads ($k = 1, \ldots 4$):

$$\frac{f_{k2}^{0,l} + f_{k2}^{1,l+1}}{F_k(\theta_w) s_{k2}(\theta_w, \mathbf{u}_w)} = \frac{f_{k8}^{0,l+1} + f_{k8}^{1,l}}{F_k(\theta_w) s_{k8}(\theta_w, \mathbf{u}_w)} = 2n_w^{1/2,l+1/2} \tag{5a}$$

$$\frac{f_{k1}^{0,l+1} + f_{k1}^{1,l+1}}{F_k(\theta_w) s_{k1}(\theta_w, \mathbf{u}_w)} = 2n_w^{1/2,l+1} \tag{5b}$$

Eqs. (5), together with the requirements that there is no mass flux perpendicular to the wall in the mixing nodes:

$$\sum_k c_k \left[f_{k4}^{1,l} + f_{k6}^{1,l+1} \right] = \sum_k c_k \left[f_{k2}^{0,l} + f_{k8}^{0,l+1} \right] \tag{6a}$$

$$\sum_k c_k f_{k5}^{1,l+1} = \sum_k c_k f_{k1}^{0,l+1} \tag{6b}$$

may be solved to get the values of the distribution functions in the ghost nodes $(0, l)$ and $(0, l+1)$ after each time step. Similar relations may be used to compute the values of the corresponding distribution functions in the ghost nodes outside the right wall of the channel.

1.2.2 Inflow/outflow boundaries

The wall temperature and velocity are set to $\theta_w = 1$ and $\mathbf{u}_w = 0$, while the pressure on the inflow and outflow boundaries are p_{in} and p_{out}, respectively. At both inflow/outflow boundaries, the x and y components of the fluid velocity are linearly extrapolated along the y direction to get the corresponding values in the ghost nodes. The linear extrapolation is used also to define the temperature values in the ghost nodes below the outflow boundary (Figure 1), while the temperature in the ghost nodes above the inflow boundary is set equal to the wall temperature θ_w, as done by other authors [36, 37, 38]. The values of the fluid density in the inflow/outflow ghost nodes are calculated according to the non-dimensionalized form of the ideal gas equation of state $p = n\theta$. Once the values of n, θ and $\mathbf{u}$ are known in the inflow/outflow ghost nodes, the values of the distribution functions in these nodes are set to the corresponding values of the equibrium distribution functions, which may be calculated according to eq. (3).

1.3 Lattice Boltzmann results: short channel

Figure 2 shows the stationary profiles of pressure, density, temperature and y component of the fluid velocity $\mathbf{u}$ in the stream direction down the central line $x = L/2$ of a short channel with $L = 0.2$, $h = 0.6$, $p_{out} = 5 \times 10^7$ and $\mathcal{P} = p_{in}/p_{out} = 3$. These profiles were recovered after 500,000 iterations with time step $\delta t = 10^{-4}$ on a square lattice with 21×63 nodes and spacing $\delta s = L/21$. We choose $\Lambda = 10^6$ to achieve the initial value $\mathrm{Kn}_{out} = 0.1$ of the Knudsen number $\mathrm{Kn} = \Lambda/nL$ [27] on the outflow boundary. The LB simulation results in Figure 2 may be compared to DSMC simulation results

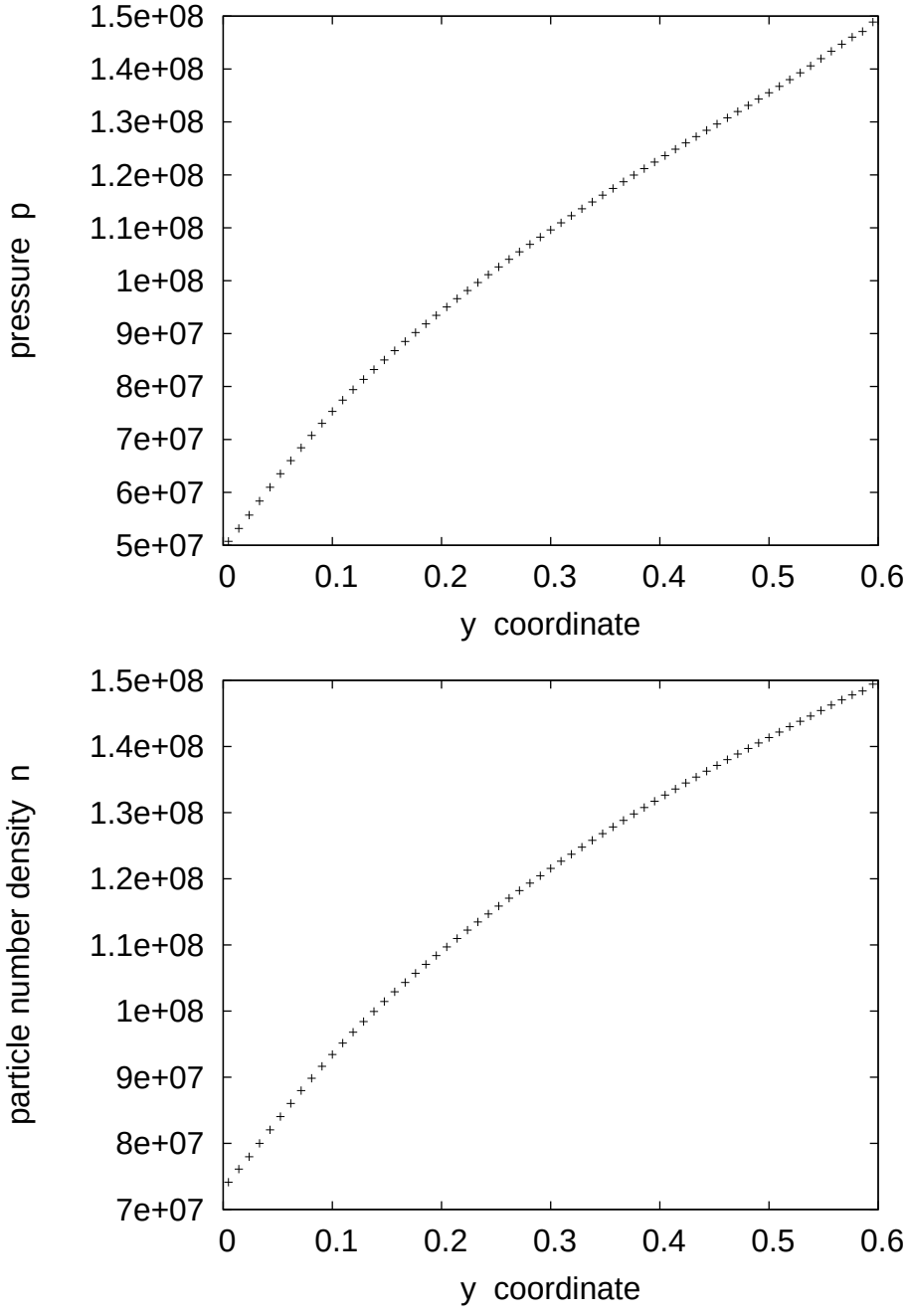

Figure 2: Stationary profiles (pressure, density, temperature and y component of the fluid velocity) in the stream direction y down the central line $x = L/2$ of a short channel ($L = 0.2$, $h = 3L$, $\mathrm{Kn}_{out} = 0.1$).

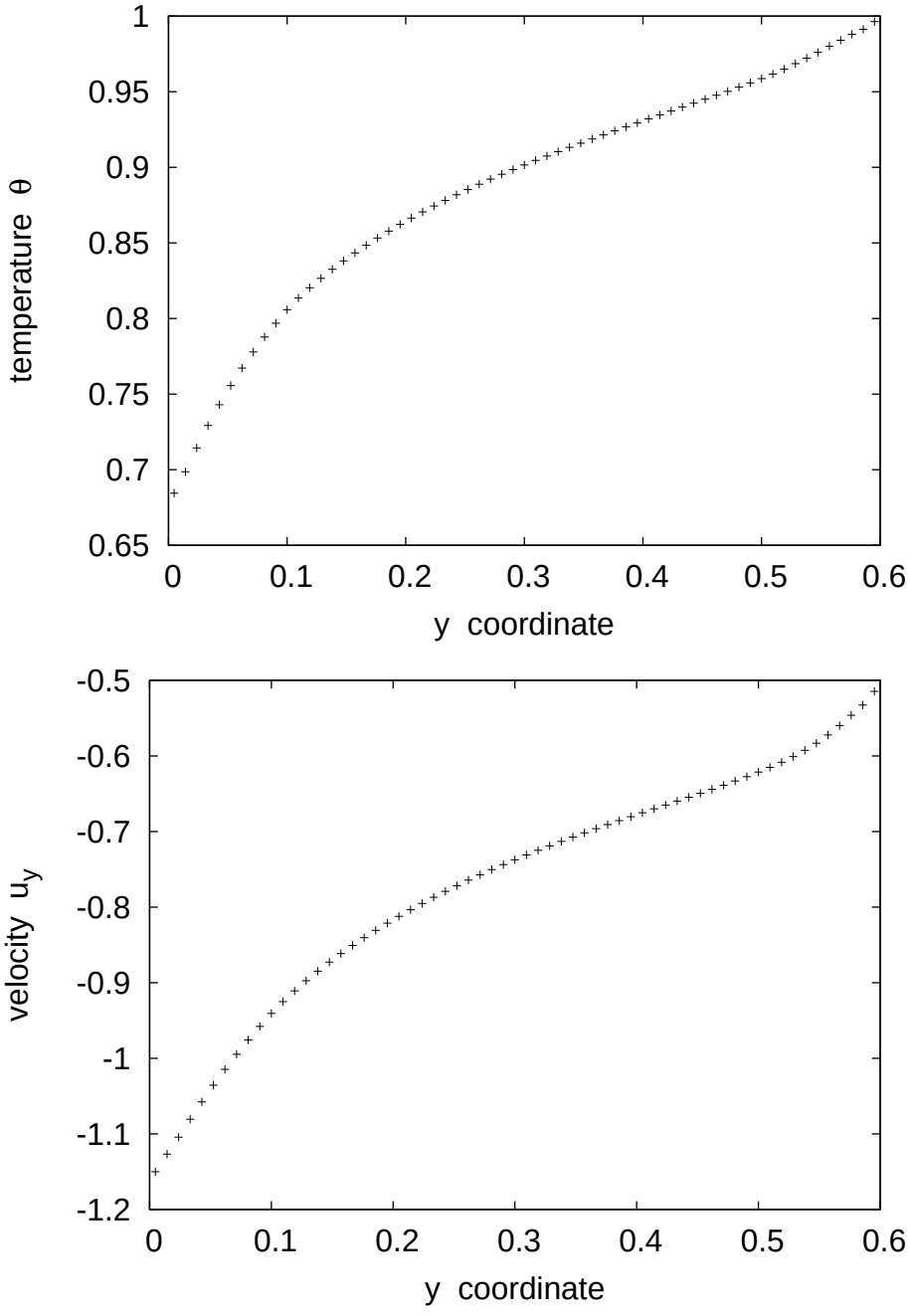

Figure 2: *(continued)* Stationary profiles (pressure, density, temperature and y component of the fluid velocity) in the stream direction y down the central line $x = L/2$ of a short channel ($L = 0.2$, $h = 3L$, $\mathrm{Kn}_{out} = 0.1$).

[36, 37, 39, 40], as well as to the BGK-Burnett solution of microchannel flow in the slip regime [38]. For this purpose, the profiles in Figure 2 should be rescaled taking into account that we used the reference values $p_0 = 10^8$, $n_0 = 10^8$, $c_s = \sqrt{2}$ and $T_0 = 1$ for pressure, density, sound velocity and temperature, while the corresponding reference values in [36, 37, 38] are $p_0 = 6.05 \times 10^{-4}$, $n_0 = 1.21 \times 10^{-3}$, $c_s = 0.91$ and $T_0 = 1$, respectively. A main characteristic of the gas flow in the short channel, which is well captured by both LB and DSMC simulations, is the large temperature drop near the ouflow boundary.

1.4 Lattice Boltzmann results: long channel

Figure 3 shows the stationary profiles of temperature and pressure in the stream direction down the central line $x = L/2$ of a long channel (21×1050 nodes) with $L = 0.2$, $h = 10$. These profiles were recovered after 2,000,000 iterations, while the other simulation paramenters remained the same as in the case of the short channel. Unlike the short channel case, the temperature variation along the long channel is less than 2%. The nonlinear presure profile along the central line, due to the competition between the compressibility and rarefection effects [7], is in good agreement with the analytical solution of Arkilic, Schmidt and Breuer [38, 41]:

$$\frac{p(y)}{p_{out}} = -6\mathrm{Kn}_{out} + \left[(6\mathrm{Kn}_{out} + \mathcal{P})^2 - (\mathcal{P} - 1)(\mathcal{P} + 1 + 12\mathrm{Kn}_{out}) \left(\frac{L - y}{L} \right) \right]^2 \qquad (7)$$

The cross-stream profiles in Figure 4 demonstrate the capability of the thermal LB model to capture also the non-vanishing velocity component normal to the walls, due to the non-uniform fluid density in the cross-stream direction [41]. As expected, the y component of the fluid velocity (whose cross-stream profile is parabolic), as well as the slip velocity at the walls (Figure 5) increase when approaching the outflow boundary, where pressure drops faster [7, 25, 41].

We investigated also the capability of the thermal LB model with diffuse reflection boundary conditions to capture the minimum of the volumic flow rate as a function of the Knudsen number. We follow [7] and express the non-dimensionalized volumic flow rate in the middle of the channel ($y = L/2$) as

$$\mathcal{Q}(y) = \frac{\bar{p} \int_0^L n(x,y) u_y(x,y) \mathrm{d}x}{-(\mathrm{d}p/\mathrm{d}y) \bar{n} L^2 c_R} \simeq constant \times \frac{\int_0^L n(x,y) u_y(x,y) \mathrm{d}x}{p_{in} - p_{out}} \qquad (8)$$

where $\bar{p}$ and $\bar{n}$ are the mean fluid pressure and density, $\mathrm{d}p/\mathrm{d}y \simeq (p_{in} - p_{out})/h$ and we took advantage of the fact that the temperature is quite constant in the channel. To achieve various values of Kn_{out}, we changed the value of p_{out} while preserving $L = 0.2$, $h = 10$, $\mathcal{P} = 3$ and $\theta_w = 1$. In Figure 6 we compare our thermal LB results with those obtained using the CLL model of Cercignani, Lampis and Lorenzani [42], as well as with the analytical solutions in the zero- and infinite-Kn limits, where $s = 1.01615$ is the slip

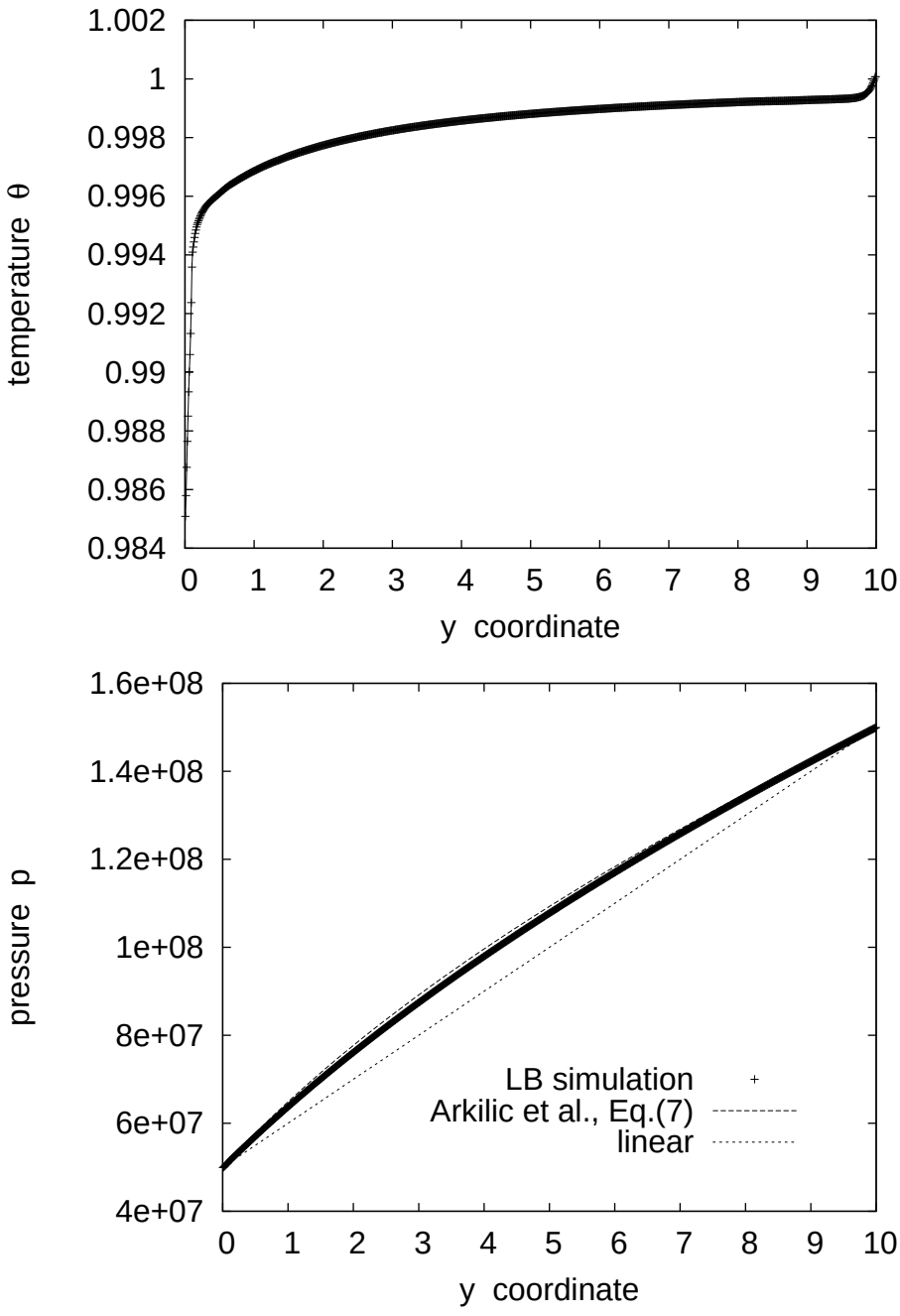

Figure 3: Stationary profiles (temperature and pressure) in the stream direction y down the central line $x = L/2$ of a long channel ($L = 0.2$, $h = 50L$, $p_{in} = 3p_{out}$, $\mathrm{Kn}_{out} = 0.1$).

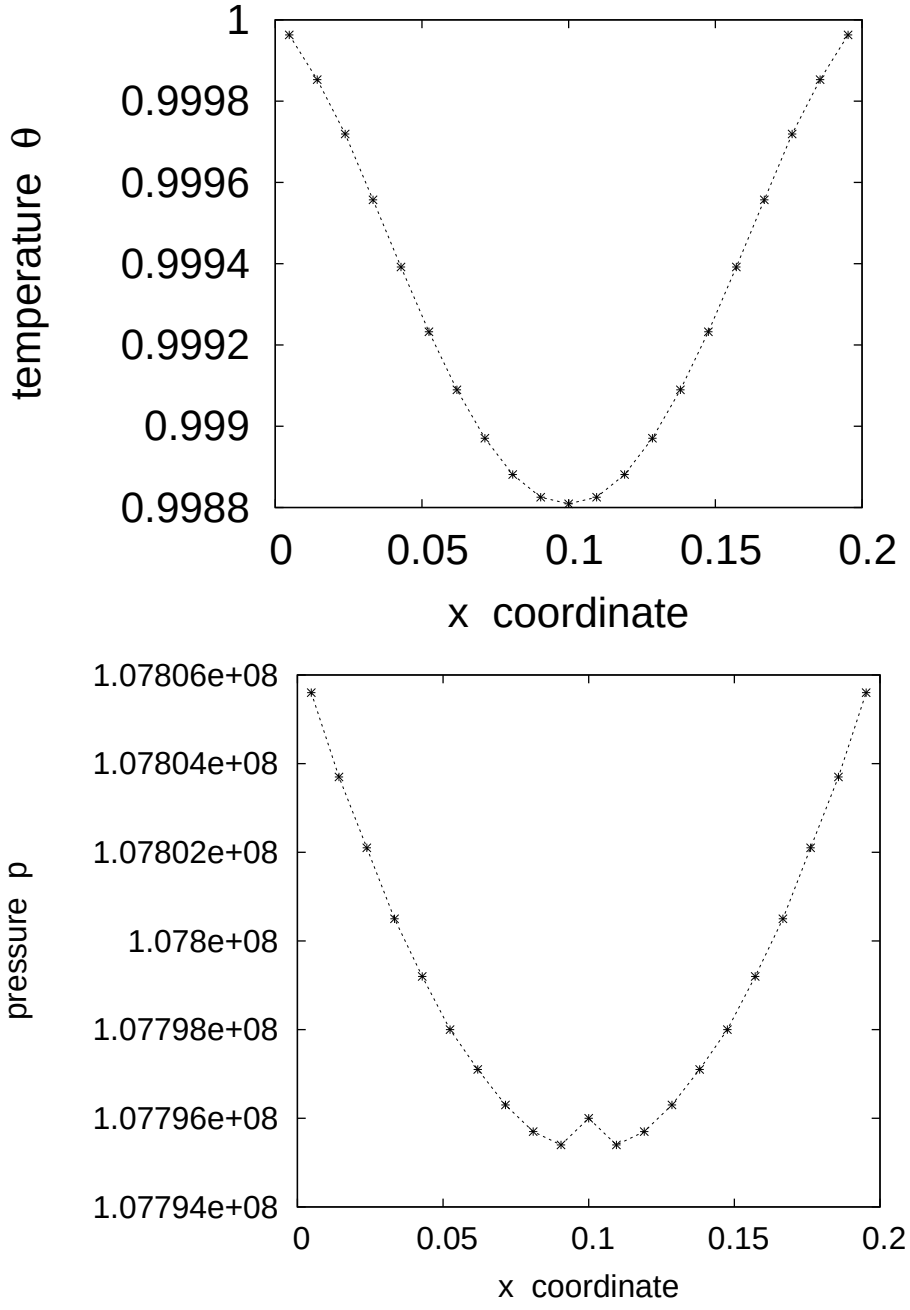

Figure 4: Stationary profiles (temperature, pressure, density and x component of the fluid velocity) in the cross - stream direction x of a long channel ($L = 0.2$, $h = 50L$, $y = L/2$, $p_{in} = 3p_{out}$, $\mathrm{Kn}_{out} = 0.1$).

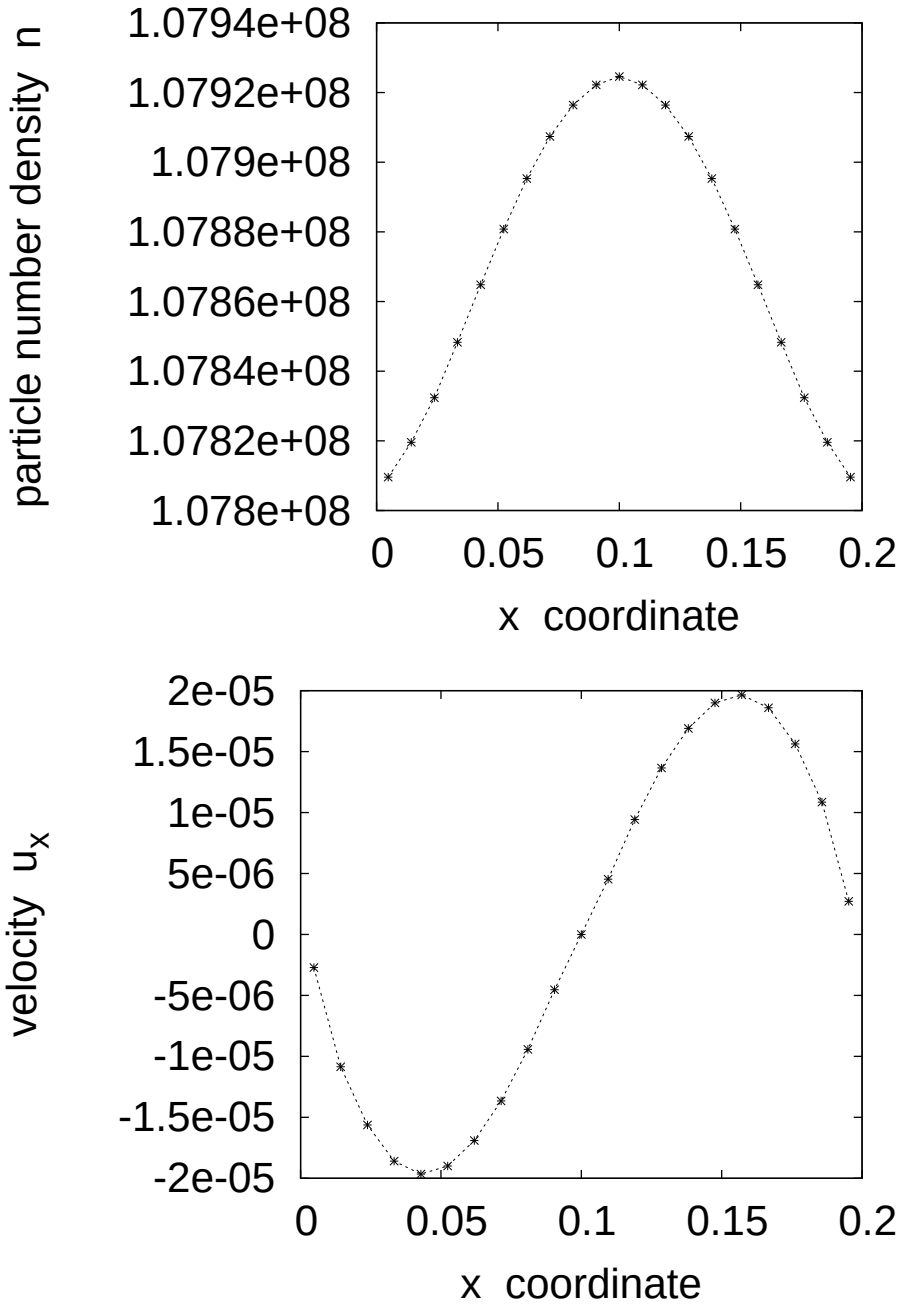

Figure 4: *(continued)* Stationary profiles (temperature, pressure, density and x component of the fluid velocity) in the cross - stream direction x of a long channel ($L = 0.2$, $h = 50L$, $y = L/2$, $p_{in} = 3p_{out}$, $\mathrm{Kn}_{out} = 0.1$).

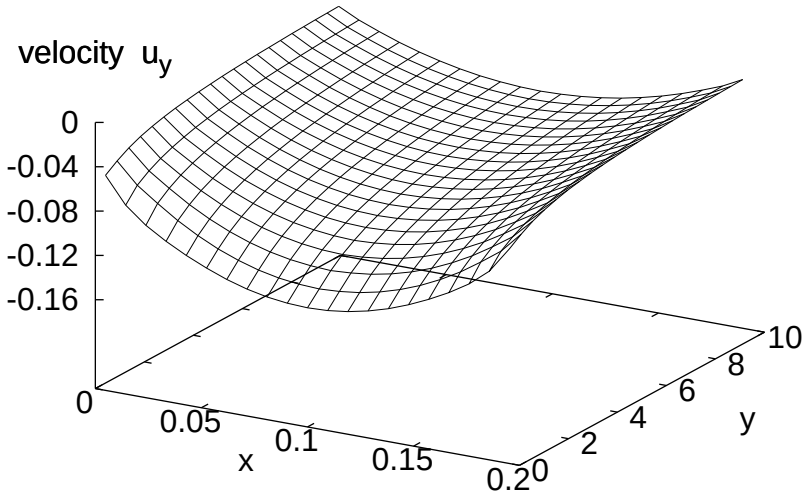

Figure 5: Stationary profile of the y omponent of the fluid velocity in the long channel.

coefficient [43]:

$$\mathcal{Q}_0 = 1/(6\mathrm{Kn}) + s + (2s^2 - 1)\mathrm{Kn} \quad (9a)$$

$$\mathcal{Q}_\infty \sim \pi^{-1/2}\log(\mathrm{Kn}) \quad (9b)$$

For $\mathrm{Kn} < 1.0$, our thermal LB results fit well to the CLL model and the minimum of the flow rate is situated around $\mathrm{Kn} = 0.625$. For larger values of Kn, the thermal LB results are situated between the analytical results predicted by eq. (9b) multiplied by a factor of 4, and those derived using the CLL model. This behaviour is very similar to the results of Toschi and Succi, recovered using an isothermal LB model for force-driven Poiseuille flow [20].

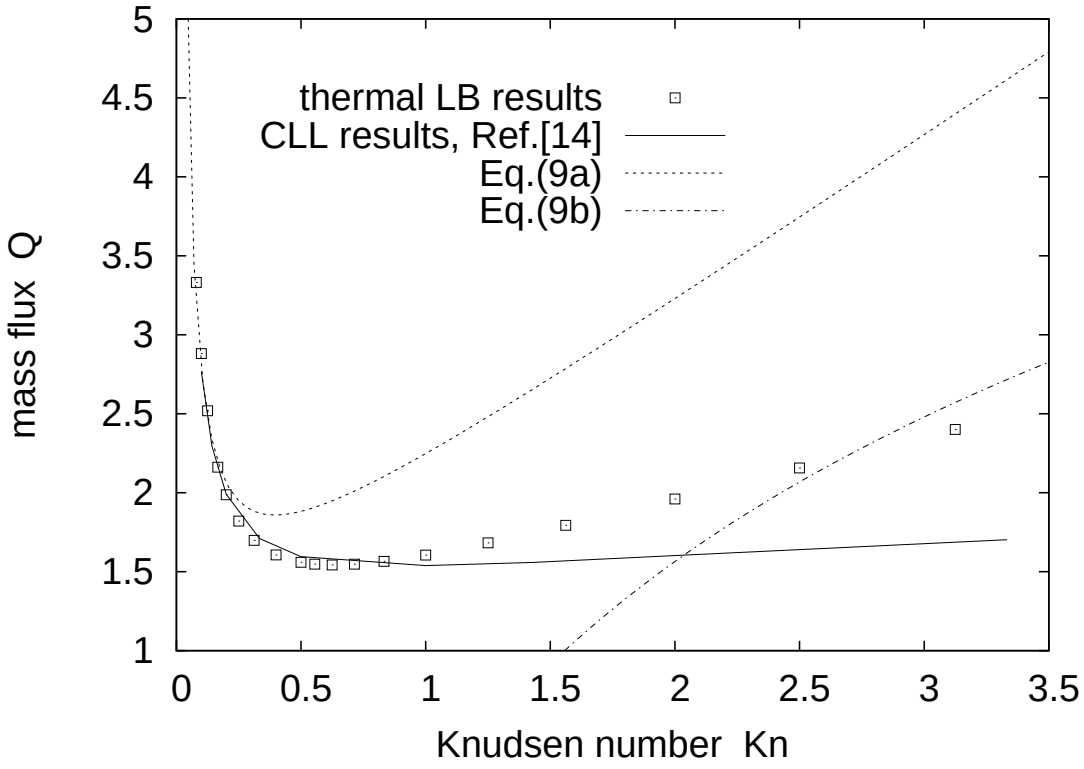

Figure 6: Normalized mass flux Q as function of Knudsen number Kn: comparison of thermal LB simulation results with calculated values in the CLL model [42], as well as with analytical solutions, Eqs.(9)

2 Force - driven microchannel flow

Let us consider the LB evolution equation with a constant external force $F_\gamma = ma_\gamma$ acting on the fluid particles of mass m [20, 23, 33, 34]

$$\partial_t f_{ki} + \mathbf{e}_{ki} \cdot \nabla f_{ki} + a_\gamma (e_{ki\gamma} - u_\gamma) f_{ki}^{eq} = -\frac{1}{\tau} [f_{ki} - f_{ki}^{eq}] \tag{10}$$

The boundary conditions on the left/right walls of the channel are the same as in Section 1.2.1 and periodic boundary conditions are considered in the vertical direction. The acceleration vector is orientated along the channel ($a_x = 0$, $a_y = a$).

Simulations were done on a 500×3 lattice with spacing $\delta s =$. We fixed the non-dimensionalized acceleration value $a = 1.0$ and the time step $\delta t = 1.0 \times 10^{-5}$. Two values of the mean fluid density were considered: $\bar{n} = 1.0 \times 10^7$ and $\bar{n} = 5.0 \times 10^7$. The corresponding values of the Knudsen number are $Kn = 0.5$ and $Kn = 0.1$, respectively. In the initial state ($iter = 0$), the fluid is at rest and begins to flow under the action of the external force. Figures 7 and 8 show the evolution of the cross-stream density, temperature, velocity and pressure profiles for both values of $\bar{n}$ mentioned above. Although the velocity profile is always parabolic, a striking feature is the occurence of the bimodal temperature profile, as well as the concave pressure profile. These features were observed also by other authors [36, 37, 38] using Direct Simulation Monte Carlo (DSMC) or BGK-Burnett solvers.

As done in the case of the pressure - driven flow, in the force - driven case we checked also the existence of the minimum of the volumic flow rate as a function of the Knudsen number. The normalized volumic flow rate is shown in Figure 9 as function of the Knudsen number. Unlike the pressure - driven case, the simulation results in the force - driven case fit well to the analytical formula, Eq. (9a), even at large values of the Knudsen number.

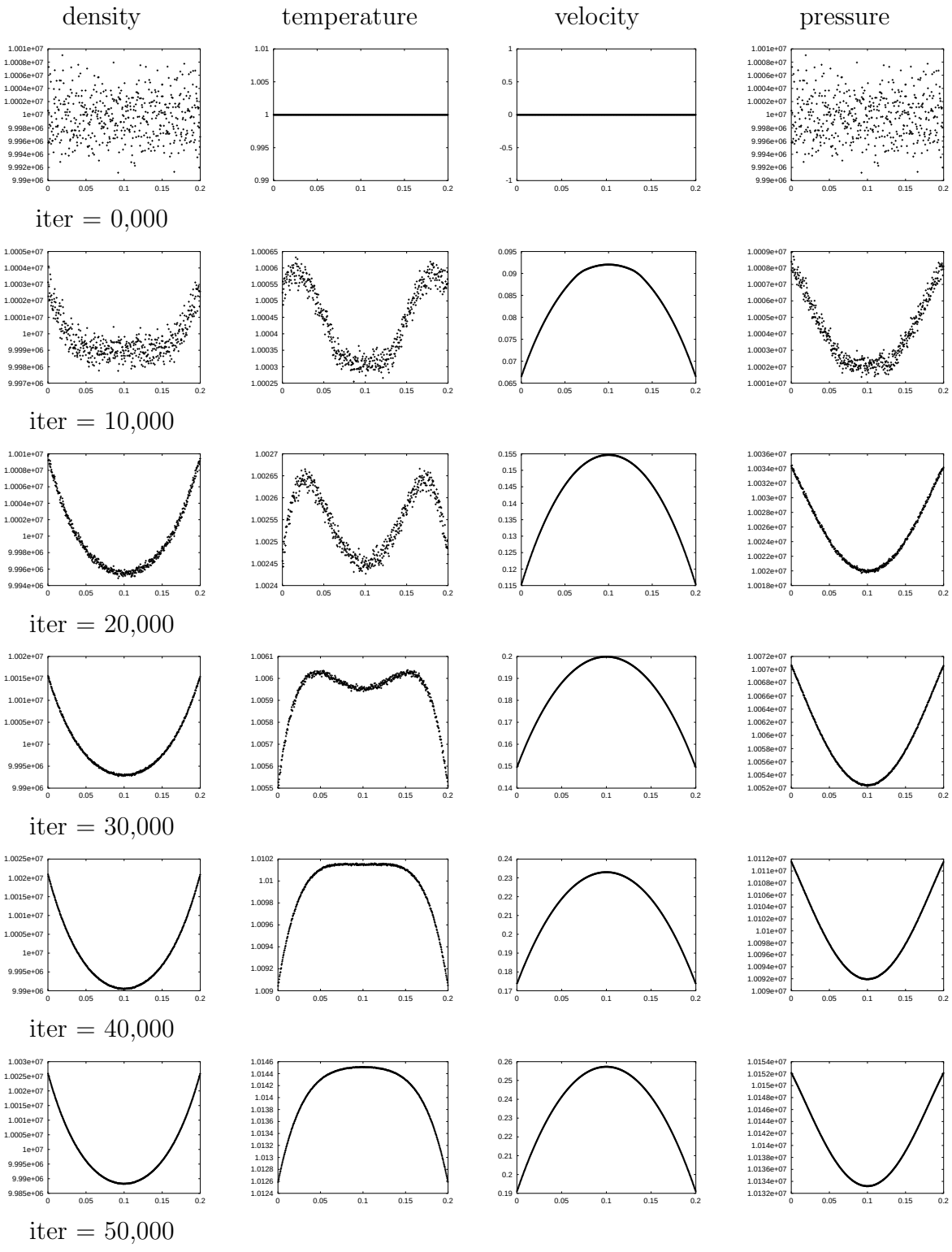

Figure 7: Evolution of density, temperature, velocity and pressure profiles in force-driven microchannel flow: $\bar{n} = 1.0 \times 10^7$, $a = 1.00$, $\delta s = 4.0 \times 10^{-4}$, $\delta t = 1.0 \times 10^{-5}$.

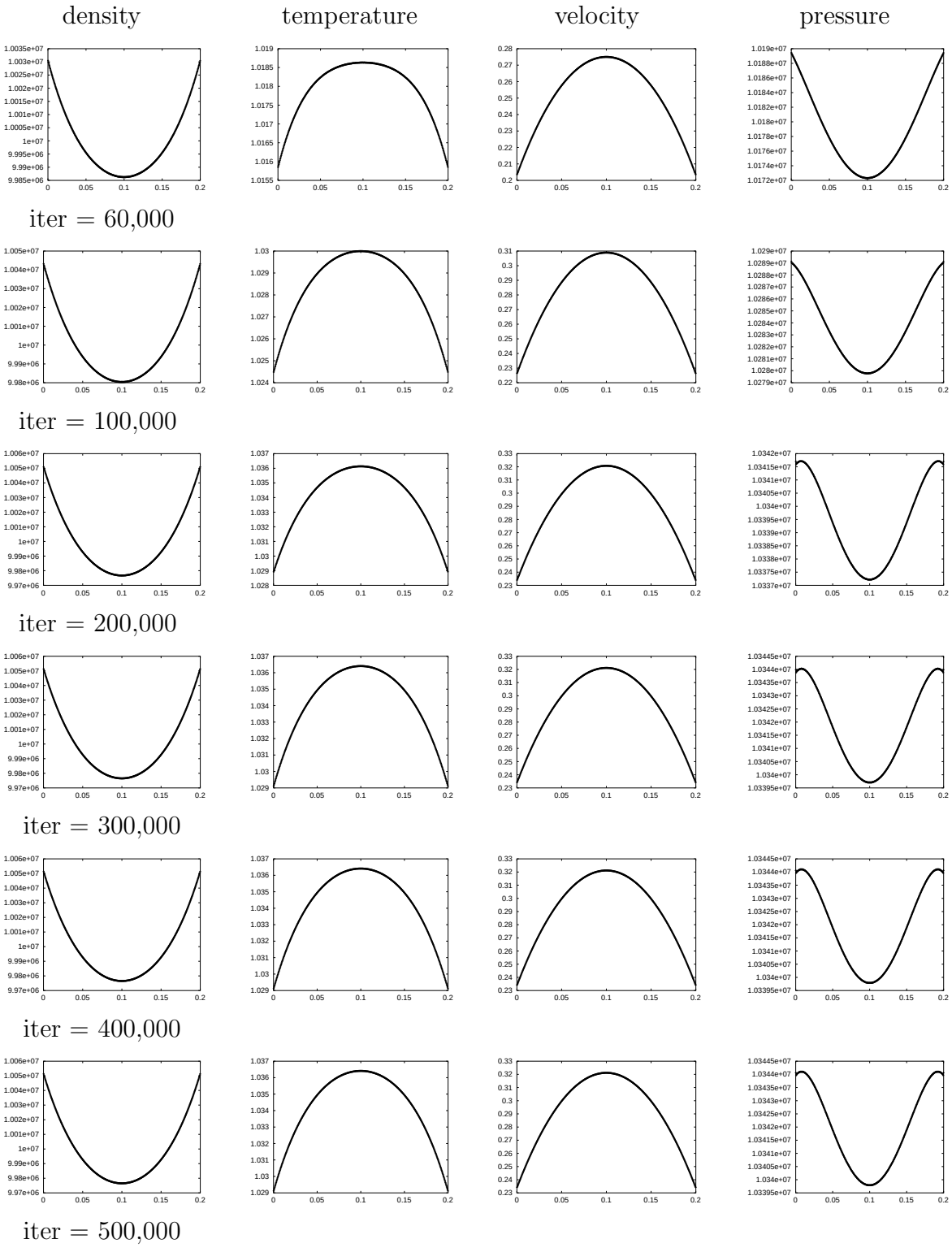

Figure 7: *(continued)* Evolution of density, temperature, velocity and pressure profiles in force-driven microchannel flow: $\bar{n} = 1.0 \times 10^7$, $a = 1.00$, $\delta s = 4.0 \times 10^{-4}$, $\delta t = 1.0 \times 10^{-5}$.

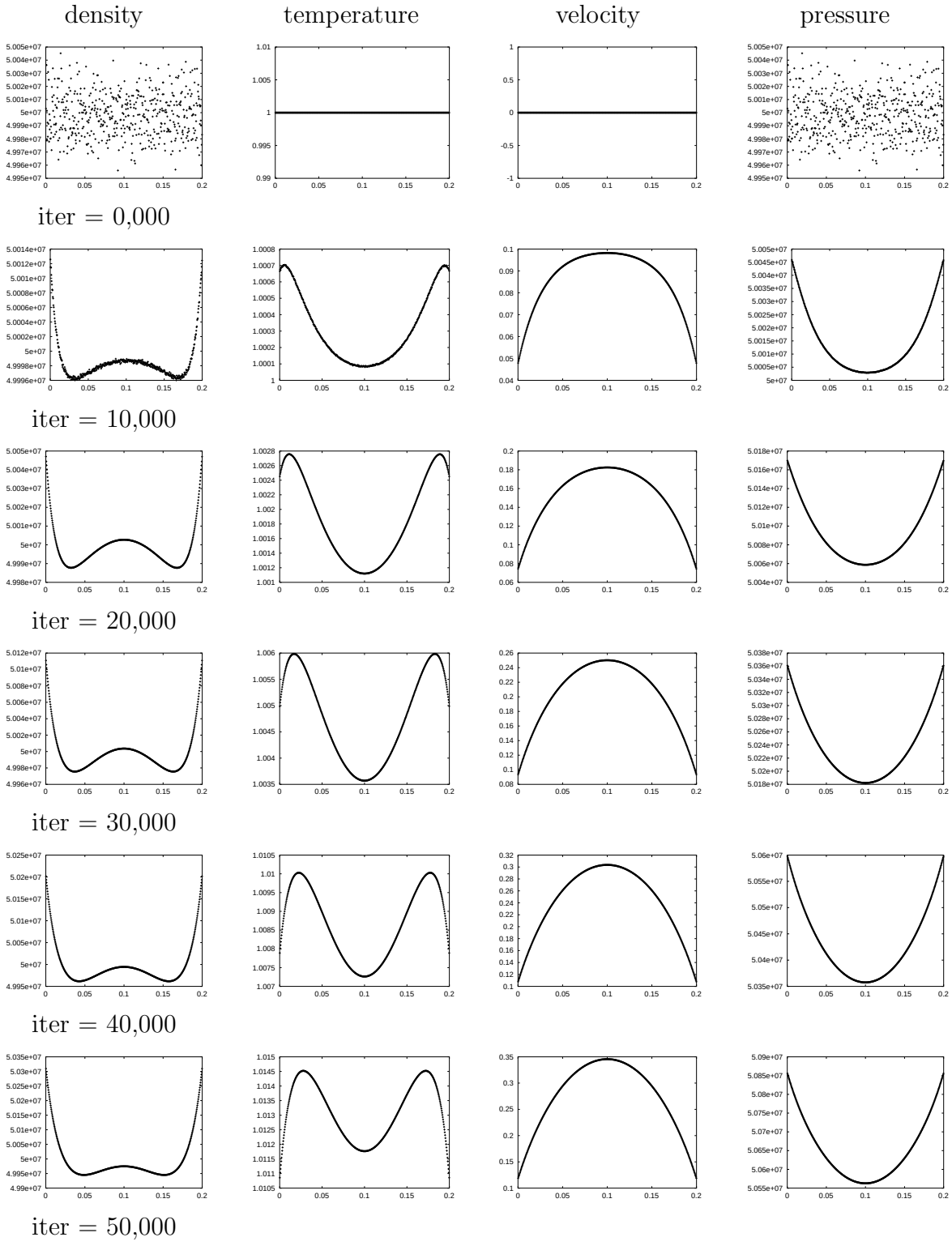

Figure 8: Evolution of density, temperature, velocity and pressure profiles in force-driven microchannel flow: $\bar{n} = 5.0 \times 10^7$, $a = 1.00$, $\delta s = 4.0 \times 10^{-4}$, $\delta t = 1.0 \times 10^{-5}$.

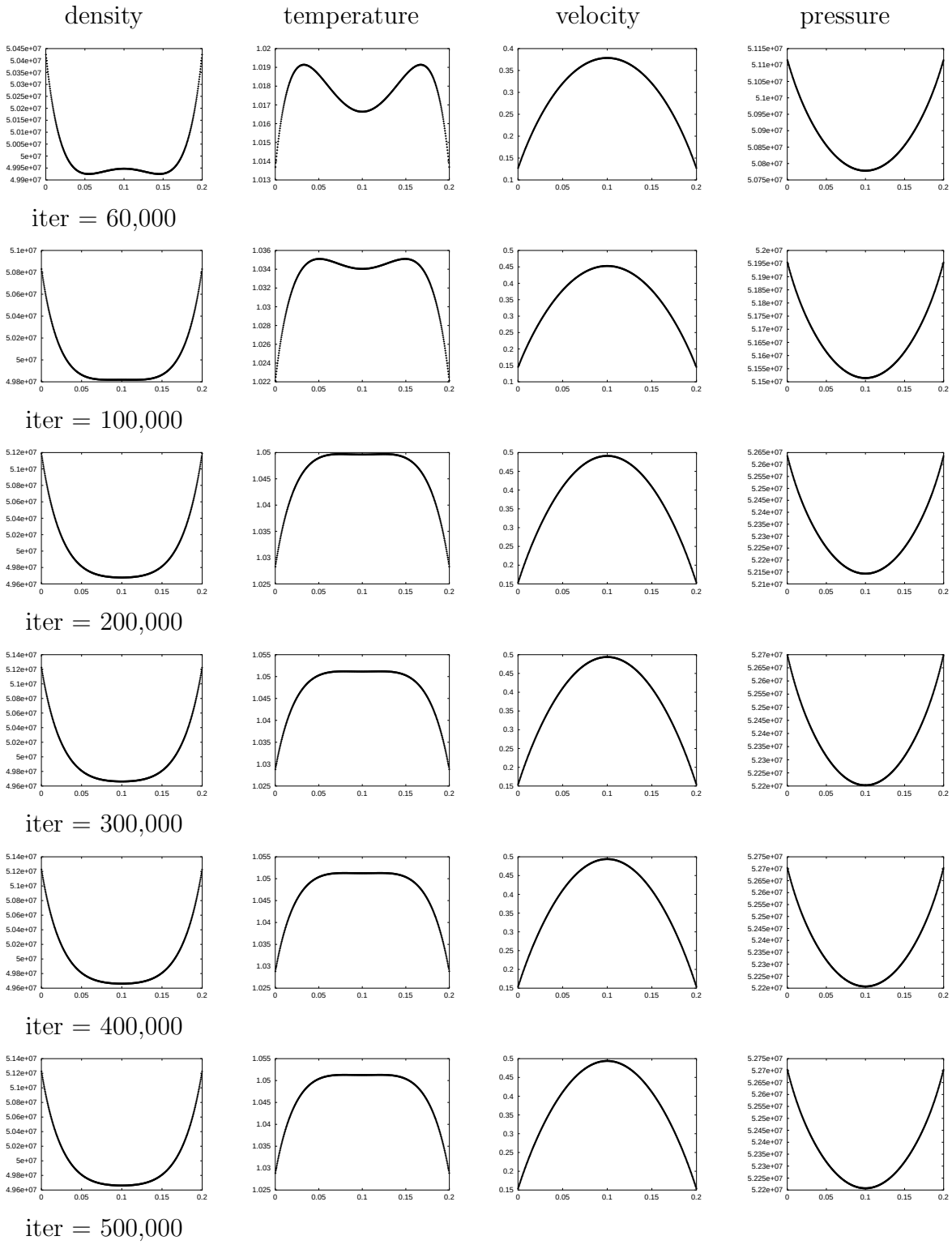

Figure 8: *(continued)* Evolution of density, temperature, velocity and pressure profiles in force-driven microchannel flow: $\bar{n} = 5.0 \times 10^7$, $a = 1.00$, $\delta s = 4.0 \times 10^{-4}$, $\delta t = 1.0 \times 10^{-5}$.

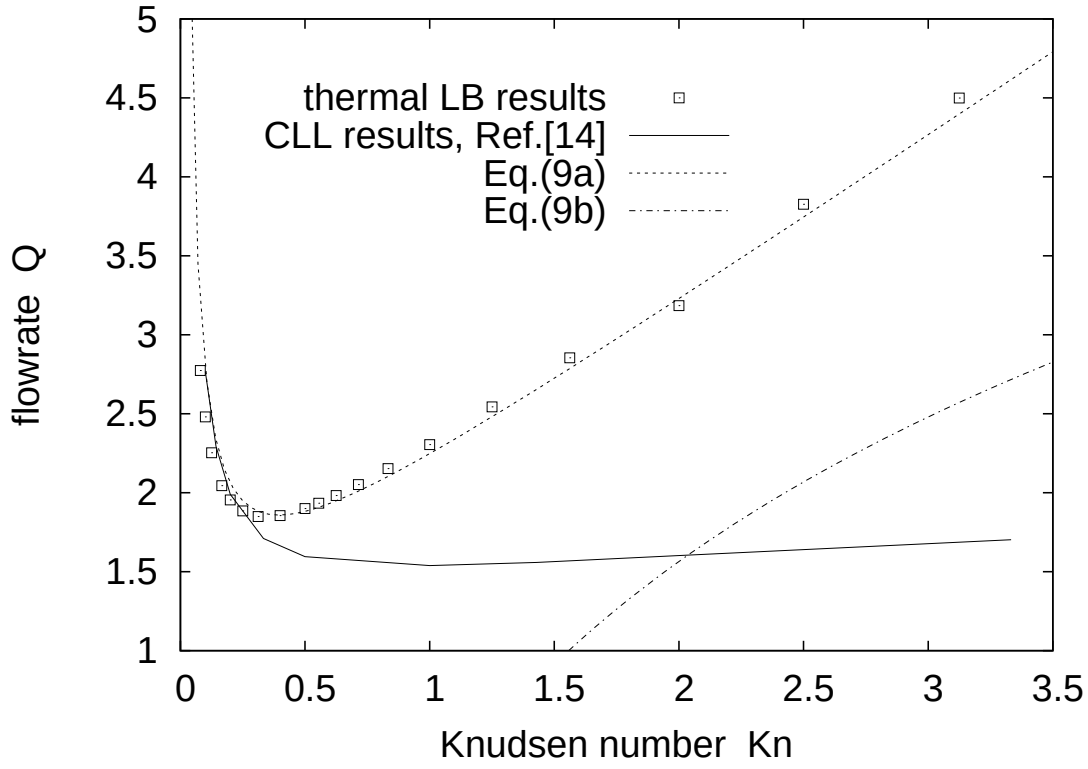

Figure 9: Normalized mass flux Q as function of Knudsen number Kn: comparison of force - driven simulation results with calculated values in the CLL model [42], as well as with analytical solutions, Eqs.(9)

3 Conclusion

We investigated the two-dimensional microchannel flow using a thermal Lattice Boltzmann model with appropriate boundary conditions. Two separate cases were considered: the pressure - driven case and the external force - driven case. A characteristics of the Lattice Boltzmann model is the recovery of the density, temperature, velocity and pressure fields from the local values of the discretized set of distribution functions, whose evolution is governed by the Boltzmann equation, which is easier to manage than the Navier - Stokes or Burnett equations.

Entrance and exit effects are present in the pressure - driven case and are clearly seen especially in the longitudinal temperature and velocity profiles when the fluid flows in a short channel. In long channels, the non-linear pressure profile along the center line, the rarefaction effects, as well as the existence of the so - called Knudsen minimum in the plot of mass flow rate vs. Knudsen number were found to be in good agreement with literature results.

References

[1] V. Sofonea and A. Cristea, *High order numerical schemes for lattice Boltzmann models: Applications to flow with variable Knudsen number*, Interim Report #0001, Contract FA8655–05–M–4008, Center of Fundamental and Advanced Technical Research, Romanian Academy – Timişoara Branch, February 28, 2005 (unpublished).

[2] V. Sofonea and A. Cristea, *High order numerical schemes for lattice Boltzmann models: Applications to flow with variable Knudsen number*, Interim Report #0002, Contract FA8655–05–M–4008, Center of Fundamental and Advanced Technical Research, Romanian Academy – Timişoara Branch, Janauary 31, 2006 (unpublished).

[3] D. H. Rothman and S. Zaleski, *Lattice Gas Cellular Automata: Simple Models of Complex Hydrodynamics*, Cambridge University Press, Cambridge, 1997.

[4] B. Chopard and M. Droz, *Cellular Automata Modeling of Physical Systems*, Cambridge University Press, Cambridge, 1999.

[5] D. A. Wolf – Gladrow, *Lattice Gas Cellular Automata and Lattice Boltzmann Models*, Springer, Berlin, 2000.

[6] S. Succi, *The Lattice Boltzmann Equation for Fluid Dynamics and Beyond*, Oxford University Press, Oxford, 2001.

[7] G. E. Karniadakis and A. Beskok, *Micro Flows: Fundamentals and Simulation*, Springer, New York, 2002.

[8] Y. Sone, *Kinetic Theory and Fluid Dynamics*, Birkhäuser, Boston, 2002.

[9] S. Colin (Editor), *Microfluidique*, Hermes Science, Paris, 2004.

[10] C. Shen, *Rarefied Gas Dynamics: Fundamentals, Simulations and Micro Flows*, Springer Verlag, New York, 2005.

[11] P. Tabeling, *Introduction to Microfluidics*, Oxford University Press, Oxford, 2005.

[12] M. Gad-el-Haq (Editor) *MEMS: Introduction and Fundamentals*, CRC Press, Boca Raton, Florida, 2005.

[13] T. M. Squires and S. R. Quake, *Microfluidics: fluid physics at the nanoliter scale*, Reviews of Modern Physics **77** (2005) 977.

[14] M. Watari and M. Tsutahara, *Two-dimensional thermal model of the finite-difference lattice Boltzmann method with high spatial isotropy*, Physical Review E **67** (2003) 036306.

[15] X. Nie, G. D. Doolen and S. Chen, *Lattice-Boltzmann simulations of fluid flows in MEMS*, Journal of Statistical Physics **107** (2002) 279.

[16] C. Lim, C. Shu, X. Niu and Y. Chew, *Application of lattice Boltzmann method to simulate microchannel flow*, Physics of Fluids **14** (2002) 2299.

[17] S. Ansumali and I. V. Karlin, *Kinetic boundary conditions in the lattice Boltzmann method*, Physical Review E **66** (2002) 026311.

[18] B. Li and D. Kwok, *Discrete Boltzmann equation for microfluidics*, Physical Review Letters **90** (2003) 124502.

[19] X. D. Niu, C. Shu and Y. T. Chew, *A lattice Boltzmann BGK model for simulation of micro flows*, Europhysics Letters **67** (2004) 600.

[20] F. Toschi and S. Succi, *Lattice Boltzmann method at finite Knudsen number*, Europhysics Letters **69** (2005) 549.

[21] T. Lee and C. Lin, *Rarefaction and compressibility effects of the lattice Boltzmann equation method in a gas microchannel*, Physical Review E **71** (2005) 046706.

[22] Y. Zhang, R. Qin and E. R. Emerson, *Lattice Boltzmann simulation of rarefied gas flows in microchannels*, Physical Review E **71** (2005) 047702.

[23] V. Sofonea and R. F. Sekerka, *Boundary conditions for the upwind finite difference Lattice Boltzmann model: Evidence of slip velocity in imcro - channel flow*, Journal of Computational Physics **207** (2005) 639.

[24] M. Sbragaglia and S. Succi, *Analytical calculation of slip flow in lattice Boltzmann models with kinetic boundary conditions*, Physics of Fluids **17** (2005) 093602.

[25] Z. Guo, T. S. Zhao and Y. Shi, *Physical symmetry, spatial accuracy and relaxation time of the lattice Boltzmann equation for microgas flow*, Journal of Applied Physics **99** (2006) 074903.

[26] R. Benzi, L. Biferale, M. Sbragaglia, S. Succi and F. Toschi, *Mesoscopic two-phase model for describing apparent slip in micro-channel flows*, Europhysics Letters **74** (2006) 651.

[27] V. Sofonea and R. F. Sekerka, *Diffuse-reflection boundary conditions for a thermal lattice Boltzmann model in two dimensions: Evidence of temperature jump and slip velocity in micro - channels*, Physical Review E **71** (2005) 066709.

[28] M. Watari and M. Tsutahara, *Supersonic flow simulations by a three-dimensional multispeed thermal model of the finite difference lattice Boltzmann method*, Physica A **364** (2006) 129.

[29] J. C. Maxwell, *On stresses in rarified gases arising from inequalities of temperature*, Philosophical Transactions of the Royal Society of London **170** (1879) 231.

[30] M. Smoluchowski, *Ueber Wärmeleitung in verdünnten Gasen*, Annalen der Physik und Chemie (Leipzig) **64** (1898) 101.

[31] W. G. Vincenti and C. H. Kruger, *Introduction to Physical Gas Dynamics* John Wiley and Sons, New York, 1965.

[32] C. Cercignani, *Rarefied Gas Dynamics: From Basic Concepts to Actual Calculations*, Cambridge University Press, Cambridge, 2000.

[33] A. Cristea and V. Sofonea, *Two component lattice Boltzmann model with flux limiters*, Central European Journal of Physics **2** (2004) 382.

[34] V. Sofonea, A. Lamura, G. Gonnella and A. Cristea, *Finite-difference lattice Boltzmann model with flux limiters for liquid-vapor systems*, Physical Review E **70** (2004) 046702.

[35] V. Sofonea and R. F. Sekerka, *Diffusivity of two-component isothermal finite difference lattice Boltzmann models*, International Journal of Modern Physics C **16** (2005) 1075.

[36] Y. Zheng, A. L. Garcia and B. J. Alder, *Comparison of kinetic theory and hydrodynamics for Poiseuille flow*, Journal of Statistical Physics *109* (2002) 495.

[37] Y. Zheng, A. L. Garcia and B. J. Alder, *Comparison of kinetic theory and hydrodynamics for Poiseuille flow*, in: Rarefied Gas Dynamics: 23rd International Symposium, Whistler, British Columbia, Canada, 20-25 July 2002, edited by A. D. Ketsdever and E. P. Muntz (AIP Conference Proceedings 663, American Institute of Physics, 2003).

[38] K. Xu and Z. Li, *Microchannel flow in the slip regime: gas-kinetic BGK-Burnett solutions*, Journal of Fluid Mechanics **513** (2004) 87.

[39] M. Malek Mansour, F. Baras and A. L. Garcia, *On the validity of hydrodynamics in plane Poiseuille flows*, Physica A **240** (1997) 255.

[40] F. J. Uribe and A. L. Garcia, *Burnett description for plane Poiseuille flow*, Physical Review E **60** (1999) 4063.

[41] E. B. Arkilic, M. A. Schmidt and K. S. Breuer, *Gaseous slip flow in long microchannels*, Journal of Microelectromechanical Systems **6** (1997) 167.

[42] C. Cercignani, M. Lampis and S. Lorenzani, *Variational approach to gas flows in microchannels*, Physics of Fluids **16** (2004) 3426.

[43] C. Cercignani, *Theory and Applications of the Boltzmann Equation*, Scottish Academic Press, Edinburgh, 1975.

[44] S. Balay, K. Buschelman, V. Eijkhout, W. Gropp, D. Kaushik, M. Knepley, L. C. McInnes, B. Smith and H. Zhang, *PETSc Users Manual*, Technical Report ANL-95/11 - Revision 2.2.1 (2004), Argonne National Laboratory, http://www.mcs.anl.gov/petsc.